

Detection of methane in air using diode-laser pumped difference-frequency generation near 3.2 μm

K. P. Petrov¹, S. Waltman², U. Simon¹, R. F. Curl¹, F. K. Tittel¹, E. J. Dlugokencky³, L. Hollberg²

¹ Departments of Electrical and Computer Engineering, and Chemistry, Rice University, Houston, TX 77251-1892, USA
(Fax: +1-713/524-5237, E-mail: FKT@rice.edu)

² Time and Frequency Division, National Institute of Standards and Technology, 325 Broadway, Boulder, CO 80303, USA

³ National Oceanic and Atmospheric Administration, 325 Broadway, Boulder, CO 80303, USA

Received: 23 June 1995/Accepted: 1 July 1995

Abstract. Spectroscopic detection of the methane in natural air using an 800 nm diode laser and a diode-pumped 1064 nm Nd:YAG laser to produce tunable light near 3.2 μm is reported. The lasers were pump sources for ring-cavity-enhanced tunable difference-frequency mixing in AgGaS₂. IR frequency tuning between 3076 and 3183 cm^{-1} was performed by crystal rotation and tuning of the extended-cavity diode laser. Feedback stabilization of the IR power reduced intensity noise below the detector noise level. Direct absorption and wavelength-modulation (2f) spectroscopy of the methane in natural air at 10.7 kPa (80 torr) were performed in a 1 m single-pass cell with 1 μW probe power. Methane has also been detected using a 3.2 μm confocal build-up cavity in conjunction with an intracavity absorption cell. The best methane detection limit observed was 12 ppb m (Hz)^{-1/2}.

PACS: 07.65; 33.00; 42.60; 42.65; 42.80

This work was done to develop a diode-laser-based technique for sensitive detection of environmentally important atmospheric trace gases such as methane, carbon monoxide, nitrous oxide, and nitric oxide. Several measurements of optical absorption in methane using tunable near-infrared lasers have been reported recently. Lucchesini et al. have used diode lasers to access $3\nu_1 + \nu_3 + (\nu_2 \text{ or } \nu_4)$ combination-overtone bands of methane near 790 nm, and the $2\nu_1 + 2\nu_3$ band near 860 nm [1]. Scott et al. have investigated the possibility of methane detection with the use of a 1.34 μm Nd:YAG laser which can access the $\nu_1 + 2\nu_3$ combination-overtone band [2]. Uehara and Tai [3] have been used a diode laser to detect methane in air by monitoring absorption in the $2\nu_3$ -stretch vibration-overtone band near 1.66 μm , achieving a detection limit of 0.3 ppm m with a signal averaging time of 1.3 s. This corresponds to 680 ppb m (Hz)^{-1/2}. Pavone and Inguscio [4] observed a component of the methane combination band corresponding to a third overtone at 866 nm.

The fundamental ν_3 band of methane near 3.2 μm , however, has transitions that are as much as a factor of 160 stronger than those of the first overtone band and may be better suited for sensitive detection. The maximum line intensity and the typical pressure broadening coefficient of methane in this band is 2.13×10^{-19} cm, and 0.027 MHz Pa⁻¹, respectively, which corresponds to a peak absorption of 0.005 m⁻¹ ppm⁻¹ in air at 1 atm near 3067 cm^{-1} [5]. Given the typical 1.8 ppm natural abundance of methane in air the absorption coefficient to be measured is 0.009 m⁻¹. The fundamental ν_3 band of methane is accessible by either conventional spectroscopy using the carbon monoxide overtone laser [6], the helium-neon laser near 3.39 μm [7], lead-salt diode lasers, color-center lasers, or with Ar⁺-dye laser difference-frequency generation [8]. These infrared laser sources are also suitable for sensitive atmospheric trace gas detection. McManus et al. [9] demonstrated an atmospheric methane measurement instrument using a Zeeman-split helium-neon laser with a sensitivity of 20 ppb with a signal averaging time of 1 s (40 ppb (Hz)^{-1/2}). Simultaneous detection of methane and other gas species in air has been accomplished with the use of a compact lead-salt diode laser spectrometer that included a multipass absorption cell [10]. A detection limit for methane of 4 ppb m near 8 μm with a signal averaging time of 3 s was reported (14 ppb m (Hz)^{-1/2}).

However, each of the mid-infrared laser sources mentioned above suffers from its own specific practical drawbacks such as large physical size, lack of portability, high cost, high power consumption, poor tunability, or need for cryogenic cooling. On the other hand, the use of commercial single-frequency short wavelength diode lasers as pump sources offers benefits of small size, reliability, low cost, and low power consumption. These diode lasers also offer good amplitude and frequency stability which are important in the design of a compact and robust gas sensor. Several new interesting diode lasers operating in the 2.7 to 3.9 μm wavelength region have been developed [11–13] but are not yet commercially available. These lasers may still require cooling with liquid nitrogen for normal operation which is sometimes a

practical drawback. Therefore, CW Difference-Frequency Generation (DFG) pumped by visible and near-infrared diode lasers at room temperature remains an attractive technique for generation of tunable mid-infrared light [14].

In this paper, the applicability of CW diode-pumped DFG to the detection of methane in air is investigated. The detection limit is based upon the measured performance characteristics of the IR probe source and detector. A significant technical difficulty in applying DFG to spectroscopic detection is its low conversion efficiency when pumped directly by most single-frequency CW semiconductor lasers. Traveling-wave semiconductor amplifiers have been successfully applied to boost effective optical pump power [15]. In earlier work [16] we reported tunable CW mid-infrared DFG with output power in excess of $3 \mu\text{W}$ pumped by relatively low-power near-infrared diode lasers. A compact ring enhancement cavity was used in order to increase effective signal power available for difference-frequency mixing.

In this work, an improved and more robust design of the build-up cavity was implemented. Direct absorption and wavelength-modulation ($2f$) spectroscopy of methane in air at 10.7 kPa (80 torr) were performed in a 1 m single-pass cell with $1 \mu\text{W}$ probe power. The detection sensitivity of $12 \text{ ppb m} (\text{Hz})^{-1/2}$ was limited by detector noise. In an effort to improve detection sensitivity, we tested the effectiveness of a confocal $3.2 \mu\text{m}$ enhancement cavity in combination with an intracavity absorption cell.

1 Diode-pumped cavity-enhanced $3.2 \mu\text{m}$ DFG source

A schematic diagram of the experimental setup is shown in Fig. 1. Two different compact lasers were used for pumping the difference-frequency IR source: a 500 mW diode-pumped monolithic Nd:YAG ring laser at 1064 nm (signal), and a 20 mW extended-cavity diode laser (ECDL) at 800 nm (pump). In later experiments, the ECDL was replaced with a 100 mW solitary laser diode in order to increase the IR power and allow fast wavelength modulation. The pump and signal laser beams were combined in a polarizing beamsplitter cube after spatial mode matching. They were then focused into a 5.5 mm antireflection-coated AgGaS_2 crystal through the input coupler of a bow-tie enhancement cavity. The cavity was designed to build up the 1064 nm light because bulk absorption in the crystal at that wavelength is lower than at 800 nm and scanning is simpler. The input coupler was a plano-concave fused silica substrate coated for high transmittance near 800 nm and 3.4% input coupling at 1064 nm. The radius of curvature of the concave side was 100 mm. The CaF_2 output coupler had the same dimensions and was coated for high reflection at 1064 nm. The transmittance of the output coupler was measured to be 41% near $3.2 \mu\text{m}$ using light from a carbon monoxide overtone laser. The long arm of the cavity was not a conventional bow-tie in that a Littrow prism reflector was used instead of a flat mirror. The function of this element was to eliminate multiple passes of the 800 nm light in the cavity. Use of a flat mirror resulted in a small portion of the diode laser

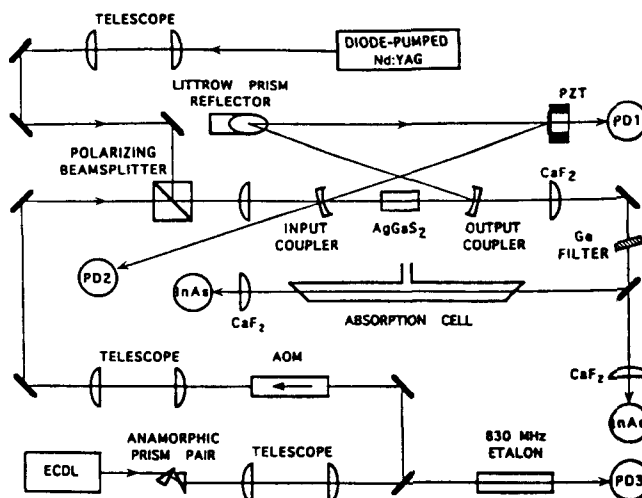


Fig. 1. Experimental setup for spectroscopic detection of methane near $3.2 \mu\text{m}$ in air. The AgGaS_2 crystal was placed into a bow-tie build-up cavity which was locked to resonance at 1064 nm. The 1064 nm light was supplied by a diode-pumped Nd:YAG laser. The tunable 800 nm light was supplied by either a grating tuned extended-cavity diode laser or a solitary laser diode. The IR power was stabilized by adjusting the diode laser power with an AOM

light circulating in the cavity which produced a systematic ripple in the IR power when the diode was tuned. The bow-tie cavity design with the addition of a Littrow prism reflector provides several advantages: it employs a minimum number of intracavity elements, is easy to align, has flexible mode diameter control, which is important for reaching optimum DFG conversion efficiency [17], and eliminates cavity resonance at the pump wavelength.

The Nd:YAG beam was spatially mode-matched to the cavity and the reflected power was monitored by a silicon photodetector PD2 (Fig. 1). Optimization of the cavity mode diameter allowed us to achieve a 90% input coupling efficiency limited mainly by the impedance mismatch of the input coupler transmittance. However, in normal operation a typical input coupling efficiency of between 75% and 85% was observed. The intracavity Nd:YAG power was monitored by a silicon photodetector PD1 which detected a 0.011% transmission through a PZT-driven flat cavity mirror (Fig. 1). The cavity build-up was 16 with the mixing crystal and 144 without. This corresponds to 6.1% and 0.7% excess cavity loss. Transmission losses in the crystal for the ordinary beam at 1064 nm have increased from 1.5% to 5.4% due to additional surface and bulk losses in the one-year time interval since the previous work [16]. Present measurements revealed 2.5% total reflection loss at 1064 nm compared to an immeasurably small reflection previously. This suggests that the index of refraction at the surface has changed. The manufacturer suggests that these changes are induced by exposure to near-UV light.

The $3.2 \mu\text{m}$ output beam (idler) was collimated by a CaF_2 lens, filtered by a broadband antireflection-coated germanium filter to remove pump and signal light, and focused by another CaF_2 lens onto a room-temperature InAs detector. A maximum of $6 \mu\text{W}$ IR power was measured with 40 mW pump power incident on the crystal, and

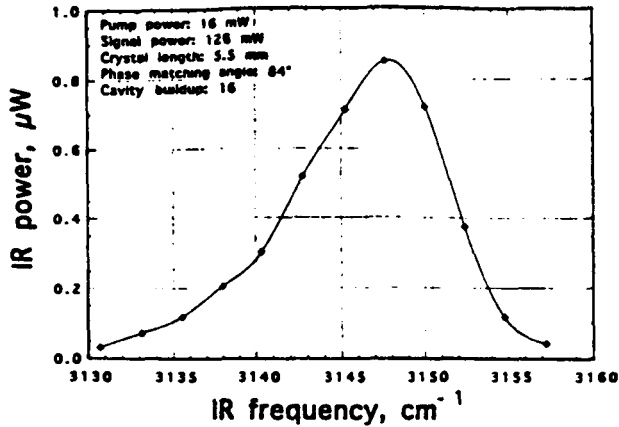


Fig. 2. Measured DFG power with pump wavelength near 800 nm for fixed phase matching angle. The full width at half maximum (FWHM) of the peak is 11 cm^{-1} . The asymmetry is a result of pumping with focused Gaussian beams

230 mW signal power in front of the cavity, which corresponds to 3.75 W intracavity signal power. Operation with more than 4.2 W intracavity Nd:YAG power was achieved, accompanied by noticeable thermal lensing in the mixing crystal. Frequency tuning of the idler wave was performed by tuning of the pump laser and crystal angle. At a fixed phasematching angle, frequency tuning over a range of approximately 10 cm^{-1} was possible as is apparent from Fig. 2. Therefore, short frequency scans of 10 GHz for spectroscopic measurements did not require crystal rotation. The observed asymmetry of the phasematching peak is a result of pumping with focused Gaussian beams [18]. Tuning of the pump laser from 801.3 nm to 795.2 nm and changing the internal phasematching angle of the crystal from 80° to 90° shifted the peak output IR power from 3076 to 3183 cm^{-1} . Operation at infrared frequencies below 3076 cm^{-1} was possible with phasematching angles below 80° but at the cost of more than 25% reduction in the output power due to larger beam walkoff, decreasing effective non-linear coefficient, and increasing Fresnel reflection losses at the AR-coated crystal surfaces which decreased the cavity build-up.

In the experiments described below the source was scanned by sweeping the frequency of the ECDL or solitary laser diode. In the ECDL, continuous mode-hop-free frequency tuning of 20 GHz was performed by electronically adjusted synchronous rotation and translation of the PZT-driven tuning mirror. The Littman configuration of the ECDL allowed tuning without steering of the output beam. The solitary laser diode was tuned by current and temperature control. Frequency scans of 10 GHz and wavelength modulation were performed by modulating the injection current. Fig. 3 shows a single-sweep $2f$ spectrum near 3086 cm^{-1} of 75.3 ppm methane in air at 13.3 kPa (100 torr) in a 59 cm single-pass cell. The spectrum was acquired by scanning the solitary diode pump laser. A low-finesse 830 MHz etalon was used for monitoring the scans.

The primary objective of the spectroscopic measurements was to determine a detection limit for methane in

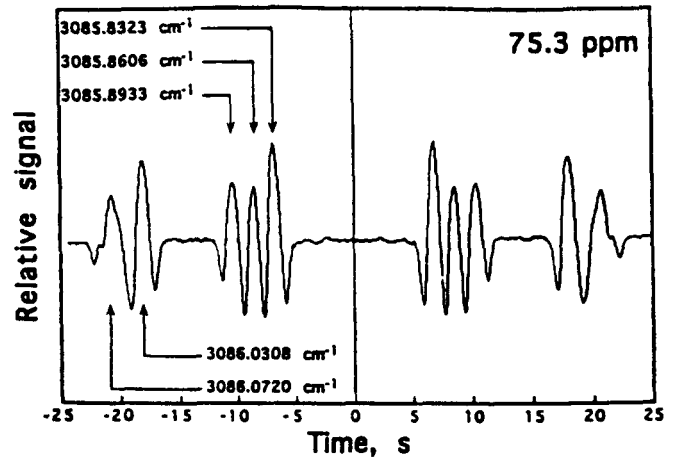


Fig. 3. Wavelength-modulation ($2f$) single-sweep spectrum of 75.3 ppm methane in 13.3 kPa (100 torr) air in a 59 cm cell. The spectrum was acquired by tuning of the solitary diode pump laser. Modulation frequency was 2 kHz, lock-in time constant was 0.1 s. The vertical solid line at the center indicates the point of sweep reversal

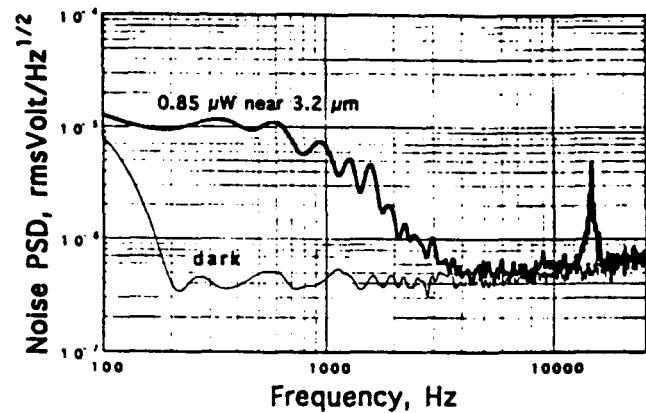


Fig. 4. The power spectral density of the noise from the InSb photo-detector/preamplifier measured with a fast Fourier transform analyzer. The upper curve was taken when the detector was exposed to $0.85 \mu\text{W}$ of IR DFG radiation near $3.2 \mu\text{m}$. Note that the buildup cavity locking noise dominates at frequencies below 3 kHz. The detector/preamplifier responsivity at $3.2 \mu\text{m}$ was $1.2 \times 10^2 \text{ VW}^{-1}$

air using light produced by difference-frequency generation pumped by tunable diode lasers and to identify the sources of noise. Figure 4 shows plots of power spectral density of the amplitude noise in the IR detector signal acquired with a fast Fourier transform analyzer. In our $2f$ spectroscopic measurements, the maximum modulation frequency of the ECDL was limited to $\sim 100 \text{ Hz}$ resulting in demodulation frequencies below 200 Hz where the cavity locking noise still dominated.

In later experiments, a servo loop was used to reduce intensity noise in the IR beam. A portion of the IR beam was focused onto a room-temperature InAs reference detector, and the feedback adjustment of the diode laser power was performed by an acousto-optic modulator. This allowed the effects of the Nd:YAG build-up cavity noise, the amplitude modulation of the diode laser result-

ing from frequency tuning, and background fringes to be cancelled out.

In addition to single-pass absorption measurements we tested the effectiveness of a confocal enhancement cavity to improve the detection sensitivity. The cavity mirrors were plano-concave quartz substrates with 250 mm radius of curvature coated for high reflection at $3.4\ \mu\text{m}$. A transmittance of 1% was measured for each mirror using a probe beam from the DFG source. The finesse of the empty cavity was measured to be 213 which suggested a 0.5% additional loss in each mirror. For spectroscopic measurements an 18 cm long absorption cell with Brewster windows was placed into the cavity, reducing the cavity finesse to 182, which corresponds to an additional loss of about 0.25% per round trip. The cavity was dither-locked to resonance at the idler wavelength by controlling a PZT-driven mirror. In order to maintain the locking when the idler frequency was tuned, the diode laser sweep and modulation signals were supplied to the PZT controller that locked the $3.2\ \mu\text{m}$ build-up cavity. Only 10% of the IR power from the DFG source could be coupled into the cavity because of poor spatial mode matching. Typical idler power delivered to the detector was only about 80 nW. With improved spatial mode matching of the IR beam, it should be possible to achieve 80% coupling into the cavity and deliver about $0.8\ \mu\text{W}$ probe power to the detector.

2 Spectroscopic detection of methane in air

Direct absorption and wavelength-modulation ($2f$) spectroscopy of both pure methane and methane in air was performed with and without IR cavity enhancement. We used three calibrated mixtures of methane with natural air; these had mixing ratios of 75.3, 10.8 and 1.8 ppm. The last was natural air sampled on a mountain ridge.

Figure 5 shows experimental wavelength-modulation ($2f$) spectra of methane in natural air sample at 13.3 kPa (100 torr) in a 59 cm single-pass cell near $3086\ \text{cm}^{-1}$. This center frequency was chosen because of the presence of six strong distinct absorption lines of methane. For example, the transition at $3085.8323\ \text{cm}^{-1}$ has a line intensity of $1.70 \times 10^{-19}\ \text{cm}$. It is only 20% weaker than the transition at $3067.3000\ \text{cm}^{-1}$ which is the strongest in the band [5]. Tuning of the source to the frequency of this strongest line was possible at the cost of reduction in IR power output. For each of the spectra, the amplitude of the frequency modulation was optimized to produce the maximum $2f$ signal size. The spectra were taken without IR power stabilization.

Figure 6 shows direct absorption spectrum of the methane in natural air at 80 torr in a 1 m single-pass cell. It was acquired using a signal-averaging bandwidth of 1 Hz, and IR power stabilization. Atmospheric pressure-broadened methane in the laboratory air between the power stabilizer beamsplitter and the sample cell is visible in the baseline trace. The baseline slope is due to interference from a secondary reflection from the power stabilizer beamsplitter. Based upon the observed signal-to-noise ratio, a detection limit (signal-to-noise ratio of 1) of $12\ \text{ppb m}(\text{Hz})^{-1/2}$ can be determined; it is in good agree-

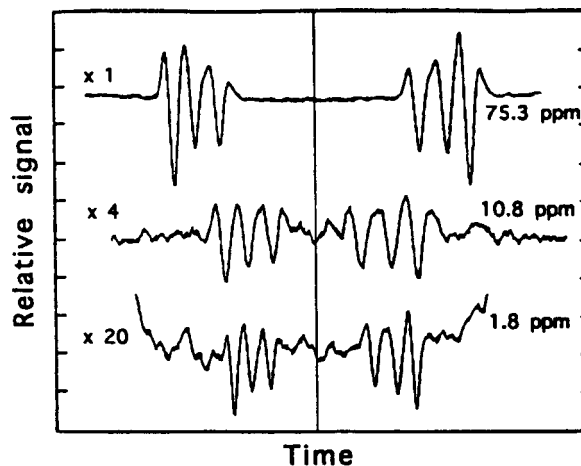


Fig. 5. Wavelength-modulation ($2f$) spectra of methane in air at 13.3 kPa (100 torr) in a 59 cm cell, obtained with $0.85\ \mu\text{W}$ of IR probe power near $3086\ \text{cm}^{-1}$. Modulation frequency was 100 Hz. Sweep times were 50 s, 50 and 500 s, and lock-in amplifier time constants were 1 s, 1 s, and 3 s, respectively. The build-up cavity locking noise can be seen in the spectrum of 1.8 ppm methane. The scan widths were not the same for the 3 traces. The traces have been offset vertically for clarity

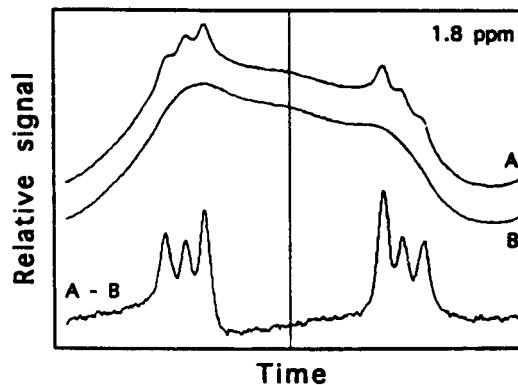


Fig. 6. Direct absorption spectrum of the methane in natural air near $3086\ \text{cm}^{-1}$ at 10.7 kPa (80 torr) in a 1 m single-pass cell (A), and the evacuated cell (B). Atmospheric pressure-broadened methane in the laboratory air between the power stabilizer beamsplitter and the sample cell is visible in the baseline trace (B). The traces have been offset vertically for clarity. Both are 2000 sweep averages resulting in 1 Hz noise bandwidth for (A-B). The detection limit of $12\ \text{ppb m}(\text{Hz})^{-1/2}$ can be inferred

ment with the measured InAs detector noise. This corresponds to an absorbance root-mean-square noise of $5.1 \times 10^{-5}\ (\text{Hz})^{-1/2}$. The detection limit can be improved. First, more IR probe power can be generated. For example, a commercial 1 W single-frequency master oscillator power amplifier (MOPA) can be used as a pump source at 800 nm. Also, a somewhat longer mixing crystal can be used. Second, better output coupler transmittance can be obtained. We have measured 60% transmittance at $3.2\ \mu\text{m}$ for the replacement output coupler and 41% for that used in the experiment. Third, an IR detector with lower noise equivalent power (NEP) can be used. The room-temperature InAs detectors used in the experiment had NEPs of $17\ \text{pW}(\text{Hz})^{-1/2}$ at $3.2\ \mu\text{m}$, which is a factor

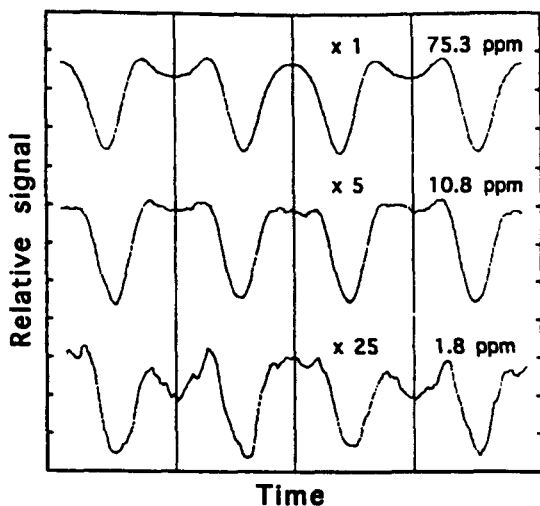


Fig. 7. Wavelength-modulation ($2f$) spectra of methane in air at 13.3 kPa (100 torr) in an 18 cm Brewster window cell inside a confocal enhancement cavity near $3.2 \mu\text{m}$. The frequency of the transition is $3086.0308 \text{ cm}^{-1}$. The detected IR power was 80 nW, sweep time was 10 s, lock-in amplifier time constant was 0.3 s. A modulation frequency of 10 Hz was used to maintain locking of the IR cavity. The IR frequency sweep range was approximately 3 GHz in order to operate with reliable locking. The traces have been offset vertically for clarity. The vertical solid lines indicate points of sweep reversal

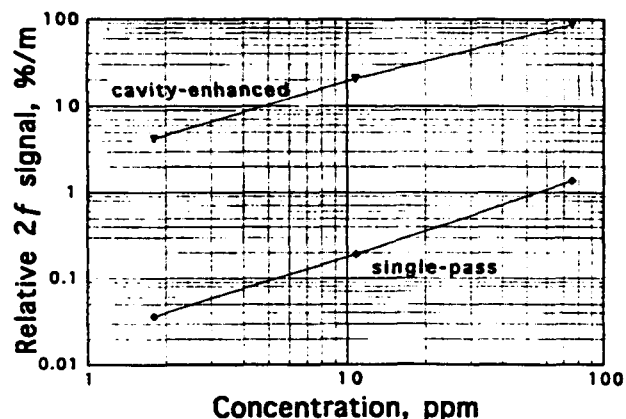


Fig. 8. Measured relative $2f$ signal amplitude per unit cell length $P_{2f}/(P_{0f}L)$ in the case of single-pass and cavity-enhanced detection, versus concentration of methane in air at 13.3 kPa (100 torr). The enhancement factor (max. 116) is in good agreement with the measured cavity finesse

of 5 larger than typical NEP of cooled InSb detectors. Fourth, either a multipass absorption cell or a build-up cavity can be used to increase effective path length.

The confocal enhancement cavity near $3.2 \mu\text{m}$ described above was used to increase the relative magnitude of the absorption signal. The effective number of passes in such cavity is

$$N = 2 \frac{F}{\pi},$$

where F is the cavity finesse, and the factor 2 accounts for two passes through an intracavity absorption cell per round trip. Given the previously measured value of cavity

finesse $F = 182$, the number of passes should be $N = 116$, which is in good agreement with the number obtained by comparing the fractional $2f$ signal per centimeter of cell length detected with cavity enhancement (Fig. 7) to that detected in the single-pass configuration (Fig. 5). The experimental enhancement factor for lower intracavity methane concentrations is in agreement with the experimental value of cavity finesse (Fig. 8). Higher concentrations of methane introduce more absorption per round trip thus decreasing the cavity finesse and the related effective number of passes which is the case with the 75.3 ppm sample.

3 Conclusion

In summary, spectroscopic detection of the methane in natural air (1.8 ppmv) using diode-laser pumped cavity-enhanced CW tunable difference-frequency generation near $3.2 \mu\text{m}$ has been performed by four methods: direct absorption spectroscopy, second-harmonic detection wavelength modulation spectroscopy, cavity-enhanced second-harmonic detection wavelength modulation spectroscopy, and direct absorption spectroscopy with power stabilization. The spectroscopic DFG source was pumped with an 800 nm diode laser and a diode-pumped 1064 nm Nd:YAG laser. It delivered a maximum of $6 \mu\text{W}$ of narrowband infrared light with 40 mW pump power and 230 mW signal power and was tunable from 3076 to 3183 cm^{-1} .

With no cryogenic components, we observed a noise equivalent concentration for the detection of methane in air at 80 torr of $12 \text{ ppb}(\text{Hz})^{-1/2}$ using a 1 m cell and direct absorption spectroscopy with power stabilization. This corresponds to an absorbance root-mean-square noise of $5.1 \times 10^{-5} (\text{Hz})^{-1/2}$. We have observed the methane in natural air at atmospheric pressure, as can be seen from the baseline trace in Fig. 6. The competing effects of increased methane density and pressure broadening compared to 80 torr cancel out so the expected detection limit would be the same.

By using an output coupler with higher transmittance, and using thermoelectrically cooled HgCdTe detectors with 5 times better noise equivalent power, we expect to be able to observe a noise equivalent column density of $1.6 \text{ ppb m}(\text{Hz})^{-1/2}$. Proper spatial mode matching into the $3.2 \mu\text{m}$ build-up cavity would yield an effective path length of 15 m and thus a predicted detection limit of $0.1 \text{ ppb}(\text{Hz})^{-1/2}$. Alternatively, a White cell could also be used. The choice of build-up cavity or multipass cell would be dictated by application-dependent constraints such as physical size and sample volume. With either the build-up cavity or a multipass cell stray interference fringes or other baseline effects may limit the actual performance before the predicted $0.1 \text{ ppb}(\text{Hz})^{-1/2}$ detection limit is reached.

Acknowledgements. The authors are grateful to Joe Wells for helping with measurements requiring the use of the carbon monoxide laser and Tamara Zibrova for the special coatings. The work was supported in part by the National Science Foundation, and the Robert A. Welch Foundation.

References

1. A. Lucchesini, I. Longo, C. Gabbanini, S. Gozzini, L. Moi: *Appl. Opt.* **32**, 5211 (1993)
2. J.C. Scott, R.A. Maddever, A.T. Paton: *Appl. Opt.* **31**, 815 (1992)
3. K. Uehara, H. Tai: *Appl. Opt.* **31**, 809 (1992)
4. F.S. Pavone, M. Inguscio: *Appl. Phys. B* **56**, 118 (1993)
5. GEISA database, Laboratoire de Meteorologie Dynamique DU C.N.R.S., Ecole Polytechnique, F-91128 Palaiseau Cedex, France
6. E. Bachem, A. Dax, T. Fink, A. Weidenfeller, M. Schneider, W. Urban: *Appl. Phys. B* **57**, 185 (1993)
7. C.B. Moore: *Appl. Opt.* **4**, 252 (1965)
8. A.S. Pine: *J. Opt. Soc. Am.* **66**, 97 (1976)
9. J.B. McManus, C.E. Kolb, P.L. Keabian: *Appl. Opt.* **28**, 5016 (1989)
10. C.R. Webster, R.D. May, C. A. Trimble, R. G. Chave, J. Kendall: *Appl. Opt.* **33**, 454 (1994)
11. H.K. Choi, G.W. Turner, Z.L. Liau: *Appl. Phys. Lett.* **65**, 2251 (1994)
12. A.N. Baranov, A.N. Imenkov, V.V. Sherstnev, Yu. P. Yakovlev: *Appl. Phys. Lett.* **64**, 2480 (1994)
13. J. Faist, F. Capasso, D.L. Sivco, C. Sirtori, A.L. Hutchinson, A.Y. Cho: *Science* **246**, 553 (April 1994)
14. U. Simon, C.E. Miller, C.C. Bradley, R.G. Hulet, R.F. Curl, F.K. Tittel: *Opt. Lett.* **18**, 1062 (1993)
15. U. Simon, F.K. Tittel, L. Goldberg: *Opt. Lett.* **18**, 1931 (1993)
16. U. Simon, S. Waltman, I. Loa, L. Hollberg, F. Tittel: *J. Opt. Soc. Am. B* **12**, 323 (1995)
17. Tran-Ba-Chu, M. Broyer: *J. Phys. (Paris)* **46**, 523 (1985)
18. G.D. Boyd, D.A. Kleinman: *J. Appl. Phys.* **39**, 3597 (1968)